Registry No. **1**, 118891-85-3; **1**-Cl_2, 118891-86-4; **1** (dimer), 118920-10-8; **4**, 128-69-8; **5**, 5521-31-3; **6**, 188-97-6; NC, 1141-38-4; AMP, 61-19-8; ATP, 56-65-5; BrdU, 59-14-3; TGAGTGAGTAAAAAAAATGAGTGCCAA, 112603-07-3; TCCTGATAAAGGAGGAGATGAAGAAAAAATGA, 118977-32-5; I^-, 20461-54-5; poly(dA), 25191-20-2; poly(rA), 24937-83-5; poly(dG), 25656-92-2; poly(dT), 25086-81-1; adenosine, 58-61-7; thymidine, 50-89-5.

References

Armstrong, R. W., Kurucsev, T., & Straus, U. P. (1970) *J. Am. Chem. Soc. 92*, 3174-3181.

Badea, M. G., & Georghiou, S. (1976) *Photochem. Photobiol. 24*, 417-423.

Berman, H. M., & Young, P. R. (1981) *Annu. Rev. Biophys. Bioeng. 10*, 87-114.

Blacker, A. J., Jazwinski, J., Lehn, J.-M., & Wilhelm, F. X. (1986) *J. Chem. Soc., Chem. Commun.*, 1035-1037.

Blacker, A. J., Jazwinski, J., & Lehn, J.-M. (1987) *Helv. Chim. Acta 70*, 1-12.

Bromley, S. D., Ward, B. W., & Dabrowiak, J. C. (1986) *Nucleic Acids Res. 14*, 9133-9148.

Dougherty, G., & Pilbrow, J. R. (1984) *Int. J. Biochem. 16*, 1179-1192.

Dourlent, M., & Hélène, Cl. (1971) *Eur. J. Biochem. 23*, 86-95.

Förster, Th. (1948) *Ann. Phys. 2*, 55-75.

Georghiou, S. (1981) *Modern Fluorescence Spectroscopy* (Wehry, E. L., Ed.) Vol. 3, pp 193-249, Plenum Press, New York.

IUPAC Commission on Photochemistry (1986) *EPA Newsl.*, 21-29.

Kapuscinski, J., & Darzynkiewicz, Z. (1984) *Proc. Natl. Acad. Sci. U.S.A. 81*, 7368-7372.

Kapuscinski, J., & Darzynkiewicz, Z. (1987) *J. Biomol. Struct. Dyn. 5*, 127-143.

Kubota, Y., & Motoda, Y. (1980) *Biochemistry 19*, 4189-4197.

Kubota, Y., Motoda, Y., Shigemune, Y., & Fujisaki, Y., (1979) *Photochem. Photobiol. 29*, 1099-1106.

Lianos, P., & Georghiou, S. (1979) *Photochem. Photobiol. 29*, 13-21.

Neidle, S., & Waring, M. J. (1983) *Mol. Aspects Anti-Cancer Drug Action 3*, 1-34.

Nielsen, P. E., Jeppesen, C., Egholm, M., & Buchardt, O. (1988) *Nucleic Acids Res. 16*, 3877-3888.

Sari, M. A., Battioni, J. P., Mansuy, D., & Le Pecq, J. B. (1986) *Biochem. Biophys. Res. Commun. 141*, 643-649.

Slama-Schwok, A., Rougée, M., Ibanez, V., Geacintov, N. E., Montenay-Garestier, T., Lehn, J.-M., & Hélène, C. (1989) *Biochemistry* (following paper in this issue).

Spassky, A., & Sigman, D. S. (1985) *Biochemistry 24*, 8050-8056.

Steiner, R. F., & Kubota, Y. (1983) *Excited States Polym.* 203-254.

Weill, G., & Calvin, M. (1963) *Biopolymers 1*, 401-417.

Zimmerman, H. W. (1986) *Angew. Chem. 25*, 115-116.

Zinger, D., & Geacintov, N. E. (1988) *Photochem. Photobiol. 47*, 181-188.

Interactions of the Dimethyldiazaperopyrenium Dication with Nucleic Acids. 2. Binding to Double-Stranded Polynucleotides†

A. Slama-Schwok,‡,§ M. Rougée,‡ V. Ibanez,‖ N. E. Geacintov,‖ T. Montenay-Garestier,‡ J.-M. Lehn,*,‡ and C. Hélène*,‡

Laboratoire de Biophysique, Muséum National d'Histoire Naturelle, 43 Rue Cuvier, 75231 Paris Cedex 05, France, Chimie des Interactions Moléculaires, Collège de France, 11 Place Marcelin-Berthelot, 75005 Paris, France, and Chemistry Department, New York University, New York, New York 10003

Received September 28, 1988

ABSTRACT: The interactions of dimethyldiazaperopyrenium dication (**1**) with DNA have been studied by spectroscopic methods: absorption, static and dynamic fluorescence, and linear dichroism. **1** binds strongly to DNA at 250 mM NaCl, with a higher affinity for G-C pairs as compared to A-T pairs. The dye fluorescence is enhanced when it is bound to A-T pairs, whereas the emission is quenched in the vicinity of G-C pairs. Evidence for intercalation has been obtained via energy transfer and linear dichroism measurements.

Inside living cells, DNA represents an important target for different types of drugs. These drugs either bind in one of the grooves of the double helix or intercalate between base pairs. Binding of drugs on DNA may affect the biological activity in several ways: structural effects related to the binding, primarily noncovalent interactions of the drugs with duplex DNA; functional effects in which kinetics of DNA-dependent enzymes may be altered; DNA damages induced by the drug redox reactions due to either thermal or photochemical processes.

Since Lerman's intercalation model (Lerman, 1961), a large number of molecules have been shown to intercalate, for example, acridines (Neidle & Waring, 1983; Dougherty & Pilbrow, 1984), anthracyclines (Aubel-Sadron & Londos-

† The Ministère des Affaires Étrangères of France is acknowledged for the attribution of a Post-Doctoral Fellowship to A.S.-S. The linear dichroism portion of this work was performed at New York University, and the support of the Department of Energy (Grant FG-0286-ER60405) is gratefully acknowledged.

‡ Muséum National d'Histoire Naturelle.

§ Collège de France.

‖ New York University.

0006-2960/89/0428-3234$01.50/0

Gagliardi, 1984), ethidium bromide (Neidle & Waring, 1983; Dougherty & Pilbrow, 1984), and some porphyrins (Pasternack et al., 1983; Kelly & Murphy, 1985; Geacintov et al., 1987). These drugs are usually planar cationic molecules with conjugated π-electron rings.

Planarity is probably required for intercalation. Most intercalators are relatively small molecules formed by three to four planar rings, comparable in size to DNA base pairs. Their long axis may thus be parallel to that of the base pairs, and a local elongation and distortion of DNA will be the major structural effect due to intercalation (Berman & Young, 1981). The overall geometry of intercalated anthracyclines, in particular daunomycin, differs from that of other drugs (Neidle & Waring, 1983; Quigley et al., 1980): its long axis is perpendicular to the base-pair long axis, the nonaromatic ring A with the sugar residue occupying the minor groove, and ring D protruding into the major groove.

Very few studies have been devoted to the binding of dicationic aromatic molecules to DNA. Dimethyldiazapyrenium was previously shown to bind to DNA and induce photochemical cleavage reactions (Blacker et al., 1986, 1987).

Here we report spectroscopic studies of the interactions of an extended dicationic molecule, dimethyldiazaperopyrenium dichloride (**1**) with double-stranded polynucleotides and duplex DNA.

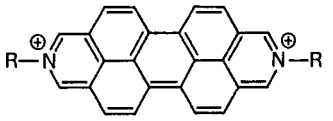

1

R = Me

Experimental Procedures

Chemicals. The chemicals used, NaCl, sodium cacodylate (dimethylarsinic acid sodium salt), HCl, KI, and KBr, were commercial (Merck) analytical reagents. The synthetic polynucleotides were P-L Biochemicals products. The calf thymus and *Clostridium perfringens* ultrapure DNA were purchased from Sigma. The synthesis of **1** has been described in the preceding paper (Slama-Schwok et al., 1989).

Apparatus. The absorption and emission apparatus have been previously described (Slama-Schwok et al., 1989). The thermal denaturation experiments were performed by using a temperature programmer connected to the thermostat, allowing a very slow temperature increase, 0.15 °C/min. In low-temperature experiments, a nitrogen flow eliminated the condensation, ensuring correct absorbance measurements. The accuracy of the results in the time scale of T_m experiments was checked by measuring the absorbance of either free polynucleotides or complexes at constant temperature during 14 h. The precision of the measurements was $\Delta OD = \pm 0.002$.

The linear dichroism measurements were performed as described (Geacintov et al., 1987) by use of a Couette cell flow gradient technique to orient the DNA.

Each apparatus was thermostated; the temperature was 20 ± 1 °C, unless otherwise stated.

Results and Discussion

Binding of Diazaperopyrenium Dication (**1**) *to Double-Stranded Polynucleotides.* (*a*) *Absorption.* Figure 1a shows the changes in absorption spectrum induced by addition of poly[d(A-T)] (0.5–500 × 10^{-6} M) to a solution of **1** (4.8 × 10^{-6} M). Two steps can be observed depending on the ratio of polynucleotide to dye (P/D): At low P/D, the absorption decreases (hypochromism), without any important wavelength

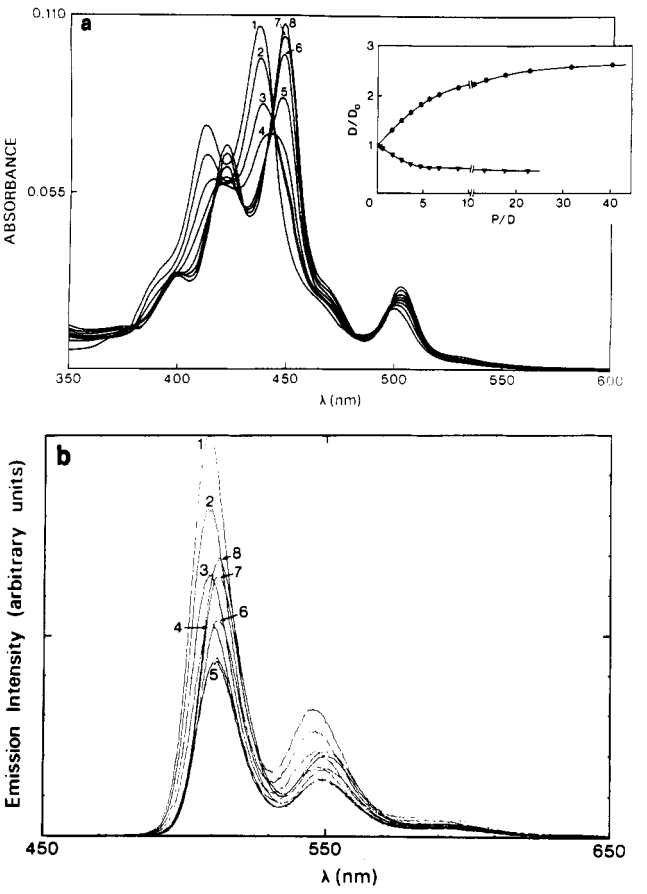

FIGURE 1: (a) Absorption study of the binding of **1** to poly[d(A-T)]. Small aliquots of concentrated poly[d(A-T)] stock solution were added to a solution containing [**1**] = 2.5 × 10^{-6} M in the presence of 0.25 M NaCl and 25 mM cacodylate buffer, pH 7.5. The final dilution was less than 10%. The light path was 1 cm. P/D = 0, 1.6, 2.6, 3.6, 5.6, 8.6, 13.4, 31.5. (Insert) Absorbance D at different P/D, relative to that of the free dye, D_0, monitored at 438 nm (triangles) and at 450 nm (circles), is corrected for dilution. (b) Fluorescence study of binding of **1** to poly[d(A-T)]. The concentration of **1** was 2.5 × 10^{-6} M. The solution was made in cacodylate buffer (25 mM) at pH 7.5 in the presence of 0.25 M NaCl. Excitation wavelength was 440 nm; excitation and emission slits were 0.6 nm. For spectra 1–8 the corresponding P/D values (expressed in units of phosphate to dye concentrations) are 0, 0.6, 1.2, 3.0, 3.6, 5.2, 8.6, and 46.4.

shift. This first step can be followed at 438 nm (see Figure 1a, insert). At higher P/D, new bands appear, red-shifted by 11 nm as compared to those of the free dye. The absorption changes at 450 nm are distinctly different from those at 438 nm (see Figure 1a, insert). The final absorption spectrum, peaking at 423, 449, and 504 nm, is similar in shape, but red-shifted as compared to that of the free dye. There are isosbestic points, at 415 and 439 nm, between the species of the first and second steps. The absorption properties of **1** bound to various double-stranded polynucleotides are compared in Table I and in Figure 2. The final absorption spectra observed with alternating and nonalternating polynucleotides, i.e., poly[d(A-T)] and poly(dA)-poly(dT) and poly[d(G-C)] (Figure 2), have very different shapes: the spectrum of **1** complexed to poly(dA)-poly(dT) resembles that obtained with single-stranded poly(dA) as far as extinction coefficients are concerned; however, it is less red-shifted than with the single-stranded polypurine (Slama-Schwok et al., 1989).

(*b*) *Fluorescence.* The changes in fluorescence spectra induced upon binding of **1** to poly[d(A-T)] are shown in Figure 1b. The binding of the dye to poly[d(A-T)] is evidenced by two processes that occur at different P/D: (1) Quenching of the dye fluorescence is observed at low P/D. (2) Enhancement

Table I: Absorption and Steady-State Fluorescence Data for **1** Bound to Different Double-Stranded Polynucleotides

polynucleotide	$D/D_0(438)^a$ hypochr	$D/D_0(450)^a$ hyperchr	ϵ $(450)^a$ (M^{-1} cm^{-1})	ϕ/ϕ_0
poly[d(A-T)]	0.45	2.76	4.25×10^4	1.20
poly[d(A-BrU)]	0.50	3.15	4.85×10^4	1.10
poly(dA)-poly(dT)	0.55	1.42	2.19×10^4	1.33
poly[d(G-C)]	0.72	3.15	4.85×10^4	0.006
poly(dG)-poly(dC)	0.49	1.51	2.32×10^4	
CT DNA	0.58	2.90	4.47×10^4	0.02
Clostridium DNA	0.50	1.74	4.35×10^4	0.10

[a] Extrapolated values for P/D = ∞.

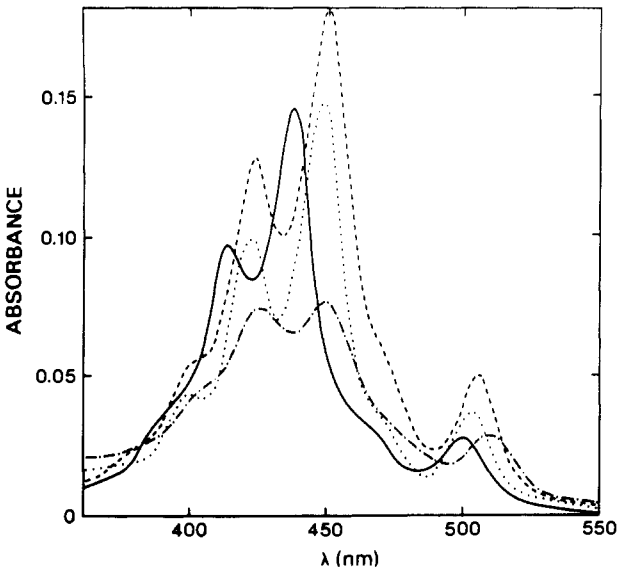

FIGURE 2: Absorption spectra of **1** free and bound to different polynucleotides. The concentration of **1** was 3.5×10^{-6} M, at pH 7.5, 25 mM cacodylate buffer, 0.25 M NaCl. P/D = 80. **1** free (solid line); **1** bound to poly[d(A-T)] (dotted line), to poly[d(G-C)] (dashed line), and to poly(dA)-poly(dT) (dot-dash line).

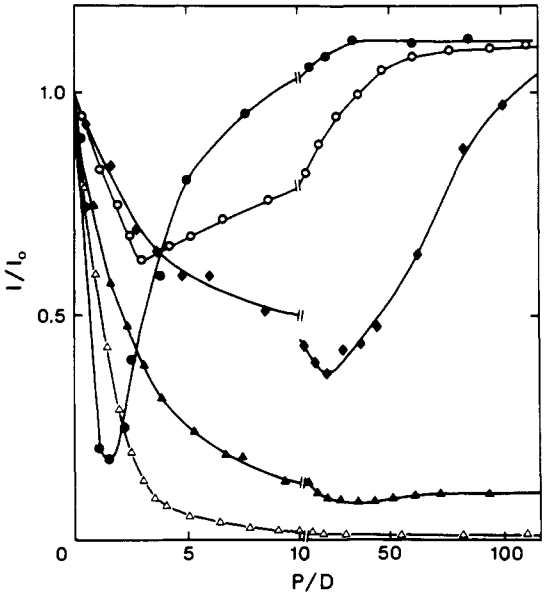

FIGURE 3: Effect of ionic concentration and of the polynucleotide sequence on the binding of dimethyldiazaperopyrenium. Fluorescence intensities I and I_0 were calculated from the integral of the emission spectra, for complexed and free **1**, and were corrected for dilution and for absorbance changes at the excitation wavelength. The absorbance was always smaller than 0.1, ensuring no deformation of the spectra. (Open circles) Binding to poly[d(A-T)], 0.25 M NaCl, 25 mM cacodylate, pH 7.5; (solid diamonds) binding to poly(dA)-poly(dT), same conditions as above; (solid circles) binding to poly[d(A-T)], 20 mM NaCl, 5 mM cacodylate buffer, pH 7.5; (solid triangles) binding to *Clostridium* DNA, 0.25 M NaCl, 25 mM cacodylate, pH 7.5; (open triangles) binding to poly[d(G-C)], same ionic strength as for DNA. In all cases, the dye concentration was in the range $(4-7) \times 10^{-6}$ M.

of the dye emission occurs at high P/D (Figure 1b).

The first step (quenching) is observed whatever the base sequence of the polynucleotide or DNA. However, there is a base-sequence dependence of the second step: the fluorescence remains quenched in the case of poly[d(G-C)]; it increases slightly in the case of DNA. At infinite values of P/D, the higher the G-C content, the higher is the quenching (see Table I and Figure 3).

The emission spectrum is red-shifted by 4–6 nm, independently of the sequence, compared to the free dye. The excitation spectrum obtained at the peak of the emission spectrum in the case of G-C-rich DNA is identical with the absorption of the bound species. Figure 3 shows the fluorescence titration curves for different double-stranded polynucleotides. The relative fluorescence quantum yields at the highest P/D are given in Table I. The emission parameters were corrected for changes of the absorption at the excitation wavelength (at 438–446 nm) and for dilution; ϕ/ϕ_0 represents the ratio of integrated emission of bound to free species. A different behavior of poly[d(A-T)] and poly(dA)-poly(dT) can be noticed in Figure 3, even though the same quantum yield is obtained with both polynucleotides at high P/D (Table I). It is known that intercalating drugs bind more tightly to poly[d(A-T)]. The weak binding to poly(dA)-poly(dT) is due to a peculiar structure of this polymer, characterized by a large propeller-twist and bifurcated H-bonds, which prevents an easy intercalation (Nelson et al., 1987). Intercalation does induce an important conformational change in poly(dA)-poly(dT) that is reflected in the cooperativity of dye binding (Wilson et al., 1985).

(*c*) *Effect of Ionic Concentration.* Figure 3 presents the comparison of fluorescence titration curves of the dye with poly[d(A-T)] at two NaCl concentrations (250 and 20 mM). The quenching is observed at lower P/D and is much more important at low ionic concentration. The increase of fluorescence intensity also occurs at lower P/D values at low ionic concentration, but the final fluorescence level is independent of ionic concentration.

Positively charged dyes, such as acridine derivatives, are known to aggregate along negatively charged polyelectrolytes such as polynucleotides (Dourlent & Hélène, 1971; Armstrong et al., 1970). Self-association of **1** has been demonstrated in the preceding paper (Slama-Schwok et al., 1989). A dimerization constant of 2×10^5 M^{-1} was estimated, which is higher than that of acridine dyes (Kapuscinski & Darzynkiewicz, 1984). Therefore, **1** is expected to stack efficiently along the polynucleotide chain. Such an aggregation should lead to a hypochromism and to a fluorescence quenching. This process is effectively observed at low P/D (Figure 3). The electrostatic attraction between the negatively charged polynucleotides and the positively charged **1** should increase at low ionic concentration. This leads to a much higher quenching efficiency

Table II: Fluorescence Data for **1** Bound to Different Double-Stranded Polynucleotides

polynucleotide	[1] × 10^{-6} M	P/D	τ_1 (ns)	B1 (%)	τ_2 (ns)	B2 (%)	τ_3 (ns)	B3 (%)	χ^2	DW
Clostridium DNA[a]	20.5	12	26.5 ± 0.2	11.9	7.3 ± 0.2	17.5	0.82 ± 0.04	70.6	1.38	1.697
	11.2	22	27.8 ± 0.2	20.8	7.6 ± 0.2	21.4	1.01 ± 0.07	57.8	1.28	1.634
	5.9	42	28.8 ± 0.3	23.6	9.1 ± 0.3	23.4	1.38 ± 0.09	53.0	1.33	1.763
	3	82	29.9 ± 0.2	24.7	9.3 ± 0.3	23.0	1.63 ± 0.08	51.3	1.13	1.486
CT DNA[a]	20.70	26.4	25.6 ± 0.4	8.4	6.3 ± 0.2	18.9	0.86 ± 0.07	72.7	0.98	1.899
			26.4 ± 0.3	9.6	7.0 ± 0.1	28.8	1.03 ± 0.05	61.6	1.15	1.829
	10.50	52.8	27.0 ± 0.3	12.0	7.60 ± 0.15	30.6	1.10 ± 0.07	57.4	1.07	1.744
	5.32	106	26.4 ± 0.3	11.0	7.33 ± 0.15	24.9	0.91 ± 0.06	64.1	1.21	1.797
CT DNA[b]	20	25	27.8 ± 0.3	10.6	7.51 ± 0.14	26.4	1.81 ± 0.07	63.0	1.36	1.581
	10	50	29.3 ± 0.5	12.5	8.9 ± 0.2	34.7	1.62 ± 0.09	52.8	1.40	1.821
	5	100	30.0 ± 0.3	14.8	8.87 ± 0.16	44.8	1.9 ± 0.1	40.4	1.12	1.895
1 alone[b]		0	26.31 ± 0.04						1.14	1.767
poly[d(A-T)][a]	6.60	16.2	33.3 ± 0.3	60.0	12.9 ± 0.7	14.0	1.2 ± 0.2	25.0	1.13	
	2.50	321	33.6 ± 0.2	92.0	8.6 ± 0.7	8.0			1.16	
	2.40	888	33.6	92.0	8.6 ± 1.6	8.0			1.44	1.600
	10.00	210	34.0 ± 0.2	90.0	9.5 ± 0.8	10.0			1.52	1.540
poly[d(A-T)][b]	10.00	210	34.6 ± 0.1	87.0	13.4 ± 0.7	13.0			1.47	1.500
	7.00	100	34.04 ± 0.14	90.0	8.5 ± 0.9	10.0			1.21	1.730
	3.00	33	34.0 ± 0.1	90.0	8.9 ± 1	10.0			1.39	1.603
N_2 saturated	3.00	33	34.6 ± 0.1	90.0	11.8 ± 0.7	10			1.15	1.700
poly[d(A-BrU)][a]	2.41	692	19.34 ± 0.08	94.0	6.8 ± 0.3	6.0			1.42	
	10.00	165	19.58 ± 0.15	87.5	10.9 ± 0.9	12.5			1.51	1.610

[a] 250 mM NaCl, 25 mM cacodylate buffer, pH 7.5. [b] 20 mM NaCl, 5 mM cacodylate buffer, pH 7.5.

under such conditions (Figure 3).

The second step, observed at high P/D, represents the binding of **1** to isolated sites on the polynucleotide (see below). An important electrostatic contribution should be invoked in this binding process as well. As a matter of fact, the conversion of **1** from external bound sites to isolated sites is more efficient at low ionic concentration.

Each binding step should be described according to the McGhee and von Hippel (1974) model, characterized by a set of three parameters: K, the association constant for binding to an isolated site; ω, the cooperativity parameter; and n, the number of base pairs covered by one ligand. The spectroscopic measurements are consistent with different locations for the aggregated and "internally bound" dye. The second step should be anticooperative if intercalation is assumed. The numerical values of K, ω, and n for the first step are difficult to obtain, since this binding is highly cooperative, and it is not "decoupled" from the second step in the concentration range available experimentally. (Adsorption phenomena lead to nonaccurate measurements at very low concentrations.)

Structural Properties. (*a*) *Effect of External Inhibitor on the "Internal" Complex of* **1** *with Poly[d(A-T)].* Approximate Stern–Volmer constants have been obtained for the quenching of dimethyldiazaperopyrenium (**1**) bound to poly[d(A-T)] by adding solid KBr to a solution at high P/D (100). Only salt concentrations in the molar range led to a measurable quenching. The Stern–Volmer constant is $K_{SV} = 0.20 \pm 0.3$ M^{-1}, which corresponds to a quenching constant $k_q = (6.6 \pm 0.8) \times 10^6$ M^{-1} s^{-1}, using an average lifetime of 30.3 ns for bound **1** (see below). This value is 3 orders of magnitude lower than the quenching constant of free **1** by KI, which is close to the diffusion-controlled value (2.0×10^{10} M^{-1} s^{-1}). The conclusion is that the diffusion of the large halide ion toward the bound dye is considerably reduced as compared to that to the free dye.

(*b*) *Fluorescence Lifetimes.* Table II summarizes typical experiments with aerated aqueous solutions of **1** in the absence and in the presence of various polynucleotides as shown in Figure 4. Best fits of the experimental points were obtained by two or three exponential component analyses of the form

$$F(t) = \sum_{i=1}^{n} B_i e^{-t/\tau_i}$$

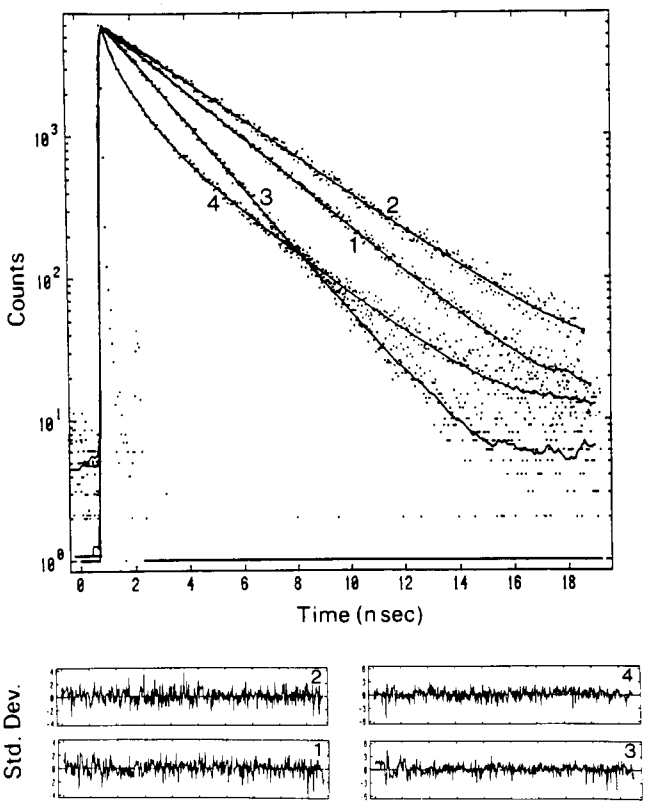

FIGURE 4: Comparison of the fluorescence decays of the dye free and bound to different polynucleotides. (1) Free dye; (2) complexed to poly[d(A-T)], P/D = 210; (3) complexed to poly[d(A-BrU)], P/D = 165; (4) bound to *Clostridium perfringens* DNA, P/D = 100. The corresponding biexponential fits are listed in Table II. The dye concentration was 1×10^{-5} M, in a solution containing 0.25 M NaCl, 25 mM cacodylate, pH 7.5. The excitation and emission wavelengths were respectively 423 and 512 nm for 1–3. Due to the low emission yield in the case of DNA, the emission monochromator was replaced by a Schott cutoff filter GG490. The excitation and emission slits were 10 nm.

(*1*) *Binding of* **1** *to Poly[d(A-T)] and to Poly[d(A-BrU)].* The first component has a longer lifetime than the free dye: 34 ns in poly[d(A-T)] as compared to 26 ns for the free dye. Its weight is up to approximately 92% at high P/D ratio (>300). This component is only little quenched by oxygen,

34.0 and 34.8 ns, respectively, in air- and nitrogen-saturated solutions. A bimolecular quenching constant $k_q(O_2) = 2 \times 10^9$ M^{-1} s^{-1} can be estimated. This figure is lower than the corresponding rate constant for quenching of the free dye by O_2, which is 7×10^9 M^{-1} s^{-1}. This is a relatively high value for an internal complex, but the aromatic rings peripherical of the dye must be accessible to oxygen, due to the large molecular size of **1**. A smaller quenching rate constant has also been obtained for the "partially" intercalated coronene, which is 5 times lower than the quenching rate constant for the free molecule (Zinger & Geacintov, 1988). This long component is attributed to an internal complex, possibly intercalated.

It should be noted that there is a large difference in the accessibility of the complexed dye to the small oxygen molecule, which remains high, and to a negatively charged halide ion, which is significantly reduced. The repulsion due to the negative electrostatic potential of double-helical polynucleotides might also explain the low quenching constant of bromide.

The long-lifetime component obtained with poly[d(A-BrU)] is noticeably shortened compared to both the free dye and the bound complex with poly[d(A-T)] (see Table II). The bromine atom of poly[d(A-BrU)], which is located in the major groove, quenches the dye fluorescence. This quenching can be explained either if the dye binds in the major groove or if the dye intercalates and protrudes into the major groove. The static quenching due to the binding of **1** to BrdU is much larger than the quenching observed with poly[d(A-BrU)] (Slama-Schwok et al., 1989). Therefore, the location of the dye does not seem to be in the major groove. If the dye is intercalated, its long axis cannot be parallel to the long axis of the base pairs because of the size of the molecule. Thus, part of **1** should protrude into the groove(s). In this case, some quenching of the fluorescence is expected if the intercalation geometry of **1** is similar to that of daunomycin (Quigley et al., 1980).

The second component has a lifetime of 8.9 ns in air-saturated solutions and 11.8 ns in the absence of oxygen. The rate constant for quenching by oxygen is difficult to calculate accurately due to the rather large error in the determination of the second component lifetime. Nevertheless, it appears that quenching is diffusion-controlled, which can be the case only if the accessibility of this complex to oxygen is large. We therefore attribute this component to an external complex. In conclusion, even at very high poly[d(A-T)] concentrations, two different species are present in the system.

(*2*) *Fluorescence Decay of Dimethyldiazaperopyrenium Bound to Poly[d(G-C)].* The fluorescence yield is too low (Table I) and does not allow quantitative lifetime measurements.

(*3*) *Fluorescence Decay of Dimethyldiazaperopyrenium* (**1**) *Bound to Calf Thymus DNA and to Clostridium perfringens DNA.* The decays required a sum of three exponentials to be satisfactorily fitted. The weight of the long-lifetime component increases with the P/D ratio and is dependent on the A-T content: it reaches 12% in calf thymus DNA (49% A-T), 25% in *C. perfringens* DNA (74.5% A-T), and 92% in poly[d(A-T)]. However, the value of the lifetime is smaller with DNA than with poly[d(A-T)]. It increases with the P/D ratio. The lower value of the long lifetime in the case of DNA as compared to that in poly[d(A-T)] may be due to internal energy-transfer processes: the fluorescence of the dye bound close to A-T base pairs (donor D) is transferred to the dye bound to G-C pairs (acceptor A), where it is quenched as demonstrated by the results obtained with poly[d(G-C)]. By use of Förster's equations (Förster, 1948), with an average orientation factor $\langle k \rangle^2 = 0.66$, a quantum yield for the dye bound to poly[d(A-T)] $\phi_D = 0.3$, a refraction index $n = 1.33$, and a calculated integral overlap $J = 4.2 \times 10^{-14}$ M^{-1} cm^3, the critical distance for energy transfer is calculated to be $R_0 = 3.7$ nm. This value corresponds to the length of a double-stranded fragment containing approximatively 11 base pairs (assuming a distance of 0.34 nm between two consecutive base pairs). Therefore, the excitation energy of **1** can be transferred from an A-T fluorescent site to a G-C quenched site with 50% efficiency when the two molecules are separated by 11 base pairs.

The second component may correspond to the external complex of poly[d(A-T)], also with energy transfer, which may explain the differences in the lifetimes with increasing P/D. The shortest lifetime is 1–2 ns; its weight decreases with increasing P/D and remains about 50% at the highest P/D. It may correspond, at low P/D, mainly to aggregates. However, since the weight of this component is still important at high P/D, it may be due to the dye located at a G-C site adjacent to an A-T base pair.

(*c*) *Base Sequence Specificity of Binding.* The fluorescence titration curve obtained with *C. perfringens* DNA (Figure 3) strongly suggests that **1** binds preferentially to G-C-rich regions. *C. perfringens* DNA contains 75% A-T. The fluorescence of **1** is quenched when it is close to a G-C base pair. The percentage of unquenching sites in *C. perfringens* DNA (two successive A-T base pairs) should be 56%. Therefore, at high P/D ratios, when energy transfer between unquenched and quenched ligands is negligible, the fluorescence of **1** should increase. This is not observed (Figure 3). This most probably reflects higher binding for G-C-rich sites, where the fluorescence is quenched. In agreement with this conclusion, the fluorescence titration curve with CT DNA ($\sim$50% A-T) is hardly distinguishable from that of poly[d(G-C)] (data not shown). A competition experiment was also carried out to demonstrate preferential binding to G-C sequences. When **1** is bound to poly[d(A-T)] at high P/D (100), its fluorescence is high (see Figure 3). Upon addition of small concentrations of poly[d(G-C)], (G-C/A-T $\sim$ 0.1), the fluorescence of **1** was quenched in a time-dependent process. A plateau was reached in about 3 min at 5 °C. The kinetics of this phenomenon was not investigated further. Nevertheless, this experiment shows that **1** binds preferentially to poly[d(G-C)] as compared to poly[d(A-T)] and is transferred from the latter to the former.

Thermal Denaturation. The thermal denaturation measurements have been performed at different ionic concentrations, 0.5 mM NaCl and 2 mM buffer or 10 mM NaCl and 1 mM cacodylate buffer, pH 7.5, by using *C. perfringens* DNA, calf thymus DNA, and poly[d(A-T)]. Typical results, monitored in the UV and in the visible, are presented in Figure 5 at low ionic concentration.

Several striking facts are noticed:

(1) The addition of **1** to poly[d(A-T)] stabilizes the double-stranded structure. The large T_m shift observed in the presence of the dye is dependent on P/D, as shown in Figure 5, and also on the A-T content of the polymer. At P/D = 10, ΔT_m of only 5 ± 2 °C and 8 ± 2 °C are obtained in the case of CT DNA and *Clostridium* DNA, respectively, whereas ΔT_m is larger than 30 °C for poly[d(A-T)]. The thermal denaturation curves are reversible, for poly[d(A-T)], within experimental error. The melting curve in the presence of the dye is less cooperative than for the polymer alone.

(2) For A-T-rich polymers, i.e., poly[d(A-T)] and *Clostridium* DNA, no change of absorption is observed when the

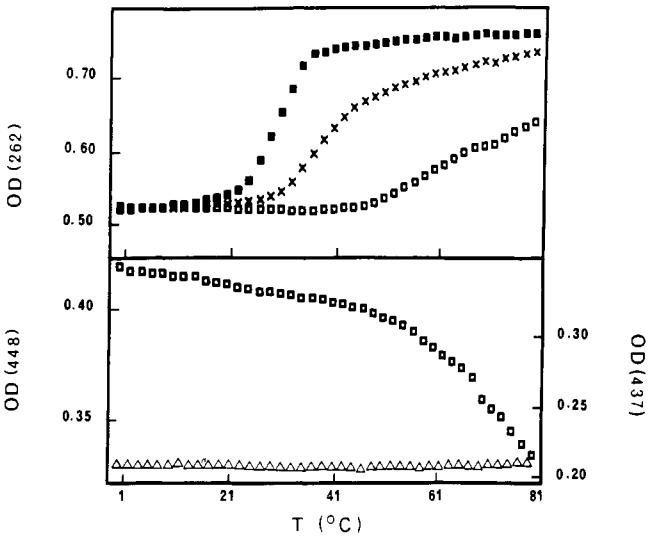

FIGURE 5: DNA thermal denaturation. This figure presents the absorbance changes in the UV and in the visible observed during one heating cycle from 0 to 80 °C using 0.5 mM NaCl and 2 mM cacodylate buffer at pH 7.5. The absorbance at 262 nm is corrected for the small contribution of the dye absorption. (Solid squares) Poly[d(A-T)] alone; (crosses) same conditions as above plus **1**, P/D = 40; (open squares) P/D = 10, same conditions as above. The OD changes in the visible at P/D = 10 were monitored at 448 nm (squares) and 437 nm (triangles), which are the maxima of bound and free **1**, respectively.

temperature is raised, at high P/D, at the maxima of the free dye (437 and 412 nm). The absorption, monitored at the maxima of the bound dye, 448 and 503 nm, decreases with increasing temperature (Figure 5).

At the P/D used and at low ionic concentration, it is known from isotherm titration that the dye is totally bound to the polymer at 20 °C. A progressive red shift of the absorption spectra is observed as the temperature is increased from 0 to 80 °C.

(3) A total or partial precipitation is observed at low P/D, typically 2–4, at very low ionic strength, independently of the nature of the polymer. This precipitation, observed also with single-stranded polynucleotides, is obtained by increasing the temperature from 0 to 80 °C, but also at 20 °C, however, at a slower rate. This phenomenon is manifested by an important decrease of the dye and polymer absorption bands. It reflects the neutralization of the negative charges of nucleic acids at low P/D.

There is no release of free dye in the bulk, upon temperature increase, as shown by the invariance of the absorbances at 437 and 412 nm, which are maxima of the free dye absorption. If **1** is released in the bulk, an increase of the absorbance at these wavelengths should be observed, due to the hypochromism induced by dye binding to ss and/or ds polymer. The red shifts of the absorption maxima in the denaturation process, when no parallel change of absorption is observed at the maxima of the free dye, are attributed to the binding of the dye to the denaturated ss. The extinction coefficient of **1** bound to ss polymers is about 2.0×10^4 M^{-1} cm^{-1}, whereas when complexed to ds, it is about 4.5×10^4 M^{-1} cm^{-1} at 448 nm. This difference explains the decrease of the absorbance monitored at 448 nm with increasing temperature if **1** binds to ss DNA after melting.

Singlet Excitation Energy Transfer. (*a*) *Poly[d(A-T)].* Overlap of the emission spectrum of DNA and the absorption spectrum of the dyes may lead to a singlet–singlet energy transfer from the bases to the dye if the distance between the DNA bases and the dye is very short. The $1/R^6$ dependence

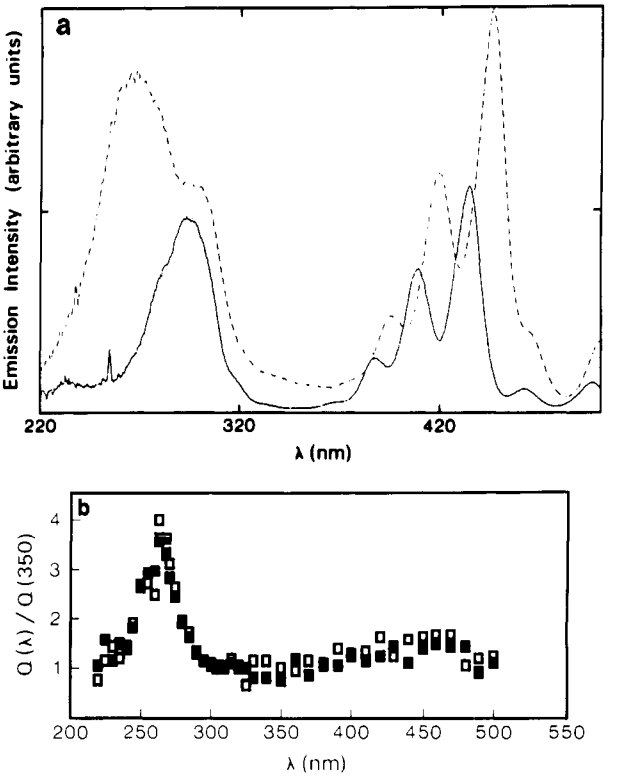

FIGURE 6: (a) Evidence for energy transfer from poly[d(A-T)] to **1**. Excitation spectra of free dye (solid line) and dye bound to poly[d(A-T)] (dotted line) are shown. Dye and poly(A-T) concentrations were 1×10^{-6} and 8.7×10^{-5} M, respectively. The buffer used was 20 mM NaCl and 5 mM cacodylate, pH 7.5. A microcell, with an optical path of $l = 0.2$ cm at the excitation and $l = 1$ cm at the emission, was used to reduce the absorbance at the excitation wavelength. The excitation spectra presented were monitored at the emission wavelength of 512 nm. (b) Enhancement of the emission of the dye bound to poly[d(A-T)], as a result of energy transfer. This figure presents the values of the ratio $Q(\lambda)/Q(350)$ as a function of the excitation wavelength (see text). The open rectangles were obtained from the data of (a), and the closed rectangles are the results obtained when the excitation spectra were recorded at the emission wavelength of 508 nm instead of 512 nm in (a).

of this process (Förster, 1948), as well as the very low fluorescence quantum yield of the bases (10^{-5}–10^{-4}), i.e., a very short excited-state lifetime in the picosecond range, implies close proximity between the donor and the acceptor for this process to occur (Morgan & Daniels, 1980; Ballini et al., 1983; Hélène, 1987). This phenomenon has been taken as evidence for intercalation: it occurs, for example, with acridine dyes, ethidium bromide, and substituted porphyrins (Weill & Calvin, 1963; Sari et al., 1986).

The excitation spectra of **1** (1×10^{-6} M) in the presence or absence of poly[d(A-T)] are presented in Figure 6a. A contribution of poly[d(A-T)] absorption to fluorescence is clearly seen around 260 nm. Energy transfer from A-T bases to bound **1** is shown by the relative quantum yield ratios of the bound dye with excitation in the UV region normalized to excitation at 350 nm, $Q(350)$, where DNA no longer absorbs, by the equation

$$Q(\mathrm{UV})/Q(350) = \frac{(I(\mathrm{UV})_b/I(\mathrm{UV})_f)(\mathrm{OD}(\mathrm{UV})_f/\mathrm{OD}(\mathrm{UV})_b)}{(I(350)_b/I(350)_f)(\mathrm{OD}(350)_f/\mathrm{OD}(350)_b)}$$

where $I(\mathrm{UV})$ represents the emission intensity observed upon excitation at a given wavelength in the UV spectral region, OD(UV) is the optical density at the same wavelength, and subscripts f and b refer to the free and the bound species (emission or absorption), respectively. The maximal ratio,

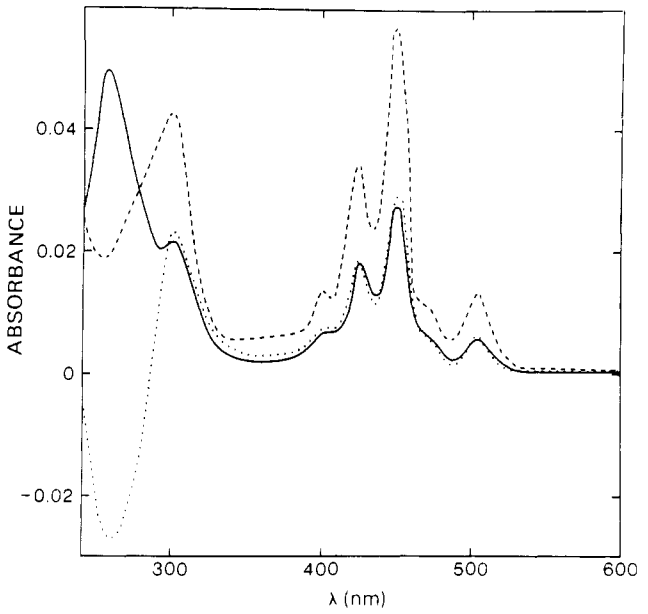

FIGURE 7: Difference absorption spectra of **1** bound to polynucleotides; effect of polymer structure. The buffer was 20 mM NaCl and 5 mM cacodylate, pH 7.5, P/D = 100. The concentration of **1** was 1.35 × 10^{-6} M. (Dotted line) Poly(dA)-poly(dT); (solid line) poly(A)-poly(U); (dashed line) poly[d(A-T)].

obtained for excitation at 262 nm, is 4 (Figure 6b).

The Förster critical distance R_0 has been calculated by assuming that the emission spectra, as well as the quantum yields, of poly(A) and poly[d(A-T)] are comparable. Under this assumption, the overlap integral is $J = 1.3 \times 10^{-14}$ M^{-1} cm^3. Using an orientation factor $\langle k \rangle^2 = 0.66$ (random orientation), $n = 1.33$, and assuming a quantum yield of fluorescence $\phi_D = 2 \times 10^{-5}$ [fluorescence quantum yield of the monomeric unit in poly(A)], the critical Förster distance is calculated to be $R_0 = 0.61$ nm. This value means that at 0.61 nm 50% energy transfer occurs if the assumptions made above are correct. A comparable R_0 value has been obtained in the case of the intercalated quinacrine (Rayner et al., 1980). If **1** is intercalated between two base pairs, then the distance between **1** and each base pair is 0.34 nm, i.e., $R_0/2$. Therefore, efficient energy transfer is expected. However it should be noted that the calculation described above involves dipole–dipole interactions. This approximation is not valid at such short distances (0.34 nm). However, this should not affect the final result, i.e., efficient energy transfer from bases to **1**.

(*b*) *Poly(dA)-Poly(dT) and Poly(A)-Poly(U).* Energy-transfer measurements have been carried out by using poly-(dA)-poly(dT) and poly(A)-poly(U) to check if intercalation is possible in these polymers, either in B or A form. The results show that the ratio $Q(UV)/Q(350)$ is close to 1 in the case of poly(A)-poly(U), whereas it is above 2 in the case of poly(dA)-poly(dT). The exact figures are difficult to obtain, since the addition of **1** to the former induces a marked hyperchromism in the absorption band of this polymer, whereas the addition to the latter induces a hypochromism (at P/D = 100), as can be seen from the difference absorption spectra presented in Figure 7. Similar difference spectra have been reported for the bound tetrapeptide lysyltryptophylglycyllysine *tert*-butyl ester (KWGK) to poly[d(A-T)] and poly(dA)-poly(dT), in which intercalation has been suggested for the tryptophyl residue (Rajeswari et al., 1987). These findings show that **1** binds preferentially to B-DNA and possibly may intercalate even in rigid poly(dA)-poly(dT) (Nelson et al., 1987).

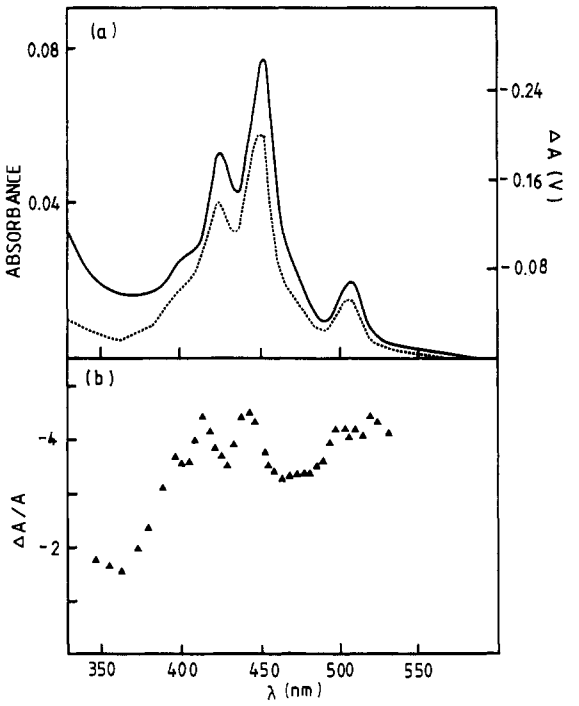

FIGURE 8: Absorption spectrum (A), linear dichroism (ΔA), and reduced dichroism ($\Delta A/A$) of the dye **1** bound to CT DNA. [DNA] = 3 × 10^{-4} M, P/D = 50, 20 mM NaCl, 5 mM cacodylate, pH 7.0. (a) Absorption spectrum (solid line) and linear dichroism spectra (dotted line) in units of volts (amplifier output). The absolute value of the linear dichroism at the maximum is −0.08. (b) $\Delta A/A$ spectrum. The reduced linear dichroism $\Delta A/A$ spectrum, in arbitrary units, has been calculated by using the data in (a).

Linear Dichroism. In a linear dichroism experiment, the DNA molecules are partially oriented, due to a velocity gradient in a Couette cell, and the absorbance of the dye bound to DNA is measured with linearly polarized light. The linear dichroism signal is defined as $\Delta A = A_{\parallel} - A_{\perp}$, where $A_{\parallel}$ and $A_{\perp}$ are the absorbances for light polarized parallel and perpendicular to the flow direction, respectively. In the case of B-DNA alone, the base pairs are nearly perpendicular to the helix axis. Molecules of DNA tend to be oriented with their helix axis parallel to the flow direction. Consequently, ΔA is negative. The orientation angle of the dye can be estimated by comparing the values of $\Delta A/A$ measured in the absorption bands of the dye with that of the DNA bases at 260 nm. If the sign and magnitude of this ratio in the visible absorption bands of the dye are the same as those of the DNA bases, then the transition moments of the dye are in the same plane as those of the base pairs, and intercalation is indicated.

Typical absorption and linear dichroism spectra, observed with the dye complexed to CT DNA, P/D = 50, are presented in Figure 8a. Negative maxima signals are observed at 506, 470 (sh), 450, 421, and 401 (sh) nm. The corresponding mean $[\Delta A/A(\text{visible})]/[\Delta A/A(260)]$, evaluated at the maximum at 450 nm, is 0.74. The corresponding $\Delta A/A$ spectrum is shown in Figure 8b, showing that the maximum deviation from the mean value, measured at the maximum absorbance, is about ±13%. The dye complexed to CT DNA at P/D = 20 and 100 give similar ratios of $[\Delta A/A(\text{visible})]/[\Delta A/A(260)]$ values (0.63 and 0.76, respectively, in 5 mM cacodylate and 20 mM NaCl, pH 7.0). Comparable values were obtained for poly[d(A-T)] and poly[d(G-C)] at low ionic concentration: 1 mM NaCl and 1 mM cacodylate (Table III). A significant increase in the linear dichroism in the polymer absorption band in the presence of **1** as compared to the values obtained in the case of dye-free polymer is observed. Because of the shape

Table III: Reduced Linear Dichroism Data for **1** Bound to Different Polynucleotides

polymer	conditions	P/D	$-\Delta A/A(260)^a$ polymer alone	$-\Delta A/A(260)^a$ polymer + dye	$-\Delta A/A(424)^a$	$-\Delta A/A(450)^a$	$-\Delta A/A(506)^a$	$\bar{r}^b$
poly[d(G-C)]	1 mM NaCl, 1 mM buffer	50	3.81	3.96	2.57	2.38	2.81	0.65
poly[d(A-T)]	1 mM NaCl, 1 mM buffer	50	0.58	0.63	0.56	0.40	0.50	0.76
poly[d(G-C)]	20 mM NaCl, 5 mM buffer	50	3.86	4.03	2.91	2.73	3.00	0.70
CT DNA	20 mM NaCl, 5 mM buffer	20	2.60	3.05	1.98	1.91	1.83	0.63
CT DNA	20 mM NaCl, 5 mM buffer	50	2.16	2.47	1.80	1.66	2.00	0.74
CT DNA	20 mM NaCl, 5 mM buffer	100	2.60	2.98	2.19	1.98	2.63	0.76

[a] Reduced linear dichroism measured at λ (nanometers) in units of volts. [b] Mean ratio of $\Delta A/A$(visible)/$\Delta A/A$(260).

of the difference LD spectrum (LD complex − LD DNA), such a large contribution of **1** to the linear dichroism can be ruled out; the difference spectrum resembles the spectrum of the polymer alone (data not shown). Such $\Delta A/A$ increases may be attributed to a stiffening or elongation of the polymer upon intercalative complex formation of a drug with the polymer (Geacintov et al., 1987).

The first transition of **1** at 506 nm corresponds to the "forbidden transition" of pyrene and is polarized along the small axis of the molecule. The second, at 450 nm, is polarized along the long axis of **1**. Both transitions present comparable $\Delta A/A$ values (Figure 8b), indicating that the plane of the bound molecule forms a mean angle of 72 ± 4° with the axis of the double helix.

On the basis of these results, one of the following three conclusions might be reached:

(1) The dye is not intercalated, but is localized in one of the grooves, most likely in the major groove due to the size of **1**.

(2) The dye destabilizes locally the B-helical structure and stabilizes a different structure in which the planes of the bases and of **1** display a comparable angle with respect to the helix axis. However, this angle is different from that of the base pairs in the unmodified portions of the DNA (which provide the main contribution to $\Delta A/A$ at 260 nm, particularly at high P/D).

(3) The dye is intercalated and causes a local distortion of the helix, due to its large size.

The first assumption can be ruled out, since an angle of 72° does not correspond to the B-DNA major groove, even within experimental error. The second hypothesis is inconsistent with the energy-transfer measurements with poly(A)-poly(U) as compared to poly(dA)-poly(dT), which show an intercalation only in B-DNA. Can the dye distort the helix? In the literature, such local geometric distortions of the helix have been reported: linear dichroism measurements of daunomycin and iremicin bound to DNA show that the mean angle between the long and the short axes and the axis of DNA are 86° and 65° for daunomycin and 62° for both axes of iremycin (Fritzsche et al., 1982). These molecules increase the length of the DNA considerably. These experimental findings have been explained as a consequence of a strong perturbation of the DNA geometry and structure resulting from the intercalation.

Linear dichroism measurements of the neutral seven-ringed coronene bound to DNA (Zinger & Geacintov, 1988) show that this large hydrocarbon molecule does not perturb the helical structure. An angle of 85 ± 3° of the coronene plane with respect to the helix axis has been found, and thus this molecule is probably inserted between adjacent base pairs. However, because of its large size, the coronene must protrude into the solvent environment and is only partially intercalated. Therefore, in the case of **1**, it is not the molecular size that seems to be the factor responsible for the perturbation of the DNA structure, but the electrostatic interactions of the charged $>NCH_3^+$ groups with DNA phosphates. The maxima of negative potential in the DNA double helix are found in the grooves (Pullman & Pullman, 1981). Therefore, it is expected that the two quaternary nitrogens are located in the major and minor grooves, respectively.

Competition Measurements. Dimethyldiazaperopyrenium bound to DNA at 0.25 M NaCl can be displaced by ethidium bromide (EB) by using a large excess of EB (EB/**1** = 85). This conclusion may be reached from the shift of the excitation maxima of **1** from 450 to 438 nm, which correspond to bound and free **1**, respectively (fluorescence measured at 512 nm). In parallel, a shift of the excitation maximum of EB from 480 to 517 nm is observed, corresponding to free and bound EB (fluorescence measured at 590 nm). Quantitative measurements of the binding constants of **1** to DNA are difficult, since energy transfer from **1** to EB has been observed, when both dyes are bound to a polynucleotide (Mergny et al., 1989).

Conclusion

Several results described above present common features with intercalating molecules: the red shifts of both the absorption and emission spectra; the enhancement of the fluorescence of the dye bound to A-T-rich polynucleotides and its quenching by G-C pairs, reminiscent of the behavior of many acridine derivatives that have been shown to intercalate; the reduced accessibility to external inhibitors (O_2 and halide); the occurrence of energy-transfer processes from poly[d(A-T)] to **1** (it has been shown that the energy-transfer efficiencies observed can be explained only if **1** is intercalated); and the competition with ethidium bromide.

In conclusion, at high ionic strength, the dimethyldiazaperopyrenium dication (**1**) *bound to double-stranded polynucleotides, at high P/D, is located mainly at an intercalating site, in which the long axis of the dye is probably perpendicular to the base pair long axis, and in part at an external site.*

The relative weights of the two complexes were estimated to be 90% and 10%, respectively, on the basis of fluorescence decay studies. These two locations may correspond to the two complexes revealed by relaxation measurements in the case of proflavin (Ramstein & Leng, 1975).

The linear dichroism measurements show a mean angle for the molecular plane of **1** to the double-helix axis of 72 ± 4°. This has been attributed to a local distortion of the DNA resulting from intercalation. The thermal denaturation experiments show that **1** may bind to denaturated DNA at high temperature, like other polycyclic aromatic hydrocarbons (Kanopa, 1983; Geacintov et al., 1976).

Binding Selectivity. The binding of the polycyclic aromatic hydrocarbons (Kanopa, 1983; Wolfe et al., 1987) and that of **1** to both native and denaturated DNA show large similarities, as mentioned above.

The binding of **1** to G-C-rich sites is much stronger than that to A-T-rich regions. The main difference between **1** and other intercalating agents is the strong stacking tendency of **1**, which induces the formation of a strong external complex along polynucleotide chains. This is due to the extended ring configuration of **1**, which leads to strong hydrophobic interactions between stacked molecules of **1**. This cooperative stacking interaction is strongly favored in the negative electrostatic field of both single-stranded and double-stranded polynucleotides.

Registry No. **1**, 118891-85-3; poly[d(A-T)], 26966-61-0; poly[d(A-BrU)], 51853-70-4; poly(dA)–poly(dT), 24939-09-1; poly[d(G-C)], 36786-90-0; poly(dG)–poly(dC), 25512-84-9.

References

Armstrong, R. W., Kurucsev, T., & Straus, U. P. (1970) *J. Am. Chem. Soc. 92*, 3174–3181.

Aubel-Sadron, G., & Londos-Gagliardi, D. (1984) *Biochimie 66*, 333–352.

Ballini, J. P., Vigny, P., & Daniels, M. (1983) *Biophys. Chem. 18*, 61–65.

Berman, H. M., & Young, P. R. (1981) *Annu. Rev. Biophys. Bioeng. 10*, 87–114.

Blacker, A. J., Jazwinski, J., Lehn, J.-M., & Wilhelm, F. X. (1986) *J. Chem. Soc., Chem. Commun.*, 1035–1037.

Blacker, A. J., Jazwinski, J., & Lehn, J.-M. (1987) *Helv. Chim. Acta 70*, 1–12.

Chaires, J. B. (1983) *Biochemistry 22*, 4204–4211.

Dougherty, G., & Pilbrow, J. R. (1984) *Int. J. Biochem. 16*, 1179–1192.

Dourlent, M., & Hélène, Cl. (1971) *Eur. J. Biochem. 23*, 86–95.

Förster, Th. (1948) *Ann. Phys. 2*, 55–75.

Fritzsche, H., Triebel, H., Chaires, J. B., Dattagupta, N., & Crothers, D. M. (1982) *Biochemistry 21*, 3940–3946.

Geacintov, N. E., Prusik, Th., & Khosrofian, J. M. (1976) *J. Am. Chem. Soc. 98*, 6444–6452.

Geacintov, N. E., Ibanez, V., Rougée, M., & Bensasson, R. V. (1987) *Biochemistry 26*, 3087–3092.

Hélène, C. (1987) *Photobiochem. Photobiophys., Suppl.*, 3–22.

Kanopa, J. (1983) *Biochem. Biophys. Res. Commun. 110*, 819–826.

Kapuscinski, J., & Darzynkiewicz, Z. (1984) *Proc. Natl. Acad. Sci. U.S.A. 81*, 7368–7372.

Kapuscinski, J., & Darzynkiewicz, Z. (1987) *J. Biomol. Struct. Dyn. 5*, 127–143.

Kelly, J. M., & Murphy, M. J. (1985) *Nucleic Acids Res. 13*, 167–184.

Lerman, L. S. (1961) *J. Mol. Biol. 3*, 18–30.

McGhee, J. D., & von Hippel, P. (1974) *J. Mol. Biol. 86*, 469–489.

Mergny, J. L., Slama-Schwok, A., Montenay-Garestier, T., & Rougée, M. (1989) *Photochem. Photobiol.* (submitted for publication).

Morgan, J. P., & Daniels, M. (1980) *Photochem. Photobiol. 31*, 101–103.

Nandi, R., Chaudhuri, K., & Maiti, M. (1985) *Photochem. Photobiol. 42*, 497–503.

Neidle, S., & Waring, M. J. (1983) *Mol. Aspects Anti-Cancer Drug Action 3*, 1–34.

Nelson, H. C. M, Finch, J. T., Luisi, B. F., & Klug, A. (1987) *Nature 330*, 211–226.

Pasternack, R. F., Gibbs, E. J., & Villafranca, J. J. (1983) *Biochemistry 22*, 2406–2414.

Pullman, A., & Pullman, B. (1981) *Q. Rev. Biophys. 14*, 289.

Quigley, G. J., Wang, H.-J., Ughetto, G., van der Marel, G., van Boom J. H., & Rich, A. (1980) *Proc. Natl. Acad. Sci. U.S.A. 77*, 7204–7208.

Rajeswari, M. R., Montenay-Garestier, T., & Hélène, C. (1987) *Biochemistry 26*, 6825–6831.

Ramstein, J., & Leng, M. (1975) *Biophys. Chem.*, 234–240.

Rayner, D. M., Szabo, A. G., Loutfy, R. O., & Yip, R. W. (1980) *J. Phys. Chem. 84*, 289–293.

Sari, M. A., Battioni, J. P., Mansuy, D., & Le Pecq, J. B. (1986) *Biochem. Biophys. Res. Commun. 141*, 643–649.

Slama-Schwok, A., Jazwinski, J., Béré, A., Montenay-Garestier, T., Rougée, M., Hélène, C., & Lehn, J.-M. (1989) *Biochemistry* (preceding paper in this issue).

Weill, G., & Calvin, M. (1963) *Biopolymers 1*, 401–417.

Wilson, W. D., Wang, Y. H., Krishnamoorthy, C. R., & Smith, J. C. (1985a) *Biochemistry 24*, 3991–3999.

Wilson, W. D., Wang, Y.-H., Kusuma, S., Chandrasekaran, S., Yang, N. C., & Boykin, D. W. (1985b) *J. Am. Chem. Soc. 107*, 4989–4995.

Wolfe, A., Shimer, G. H., Jr., & Meehan, Th. (1987) *Biochemistry 26*, 6392–6396.

Zinger, D., & Geacintov, N. E. (1988) *Photochem. Photobiol. 47*, 181–188.